

**EFFECT OF HALL CURRENTS ON CONVECTIVE HEAT
TRANSFER FLOW IN A VERTICAL WAVY CHANNEL
WITH QUADRATIC DENSITY TEMPERATURE
VARIATION**

K.Satyanarayana*

Dr. Y. Rajendra Prasad*

ABSTRACT

The effect of non-linear density temperature variation on convective heat transfer flow of a viscous electrically conducting fluid in a vertical wavy channel under the influence of an inclined magnetic field with constant heat sources. The walls of the channels are maintained at constant temperature. The equations governing the flow and heat solved by employing perturbation technique with the slope δ of the wavy wall as a perturbation parameter. The velocity and temperature distributions are investigated for different values of G , M , m , β , α , γ and λ . The rate of heat transfer is numerically evaluated for different variations of the governing parameters.

KEYWORDS: Hall Currents, Heat Transfer, Quadratic Density Temperature, Vertical Wavy Channel

* *S.S.B.N. Degree & P.G. College, Anantapur-515003, A.P. India*

INTRODUCTION

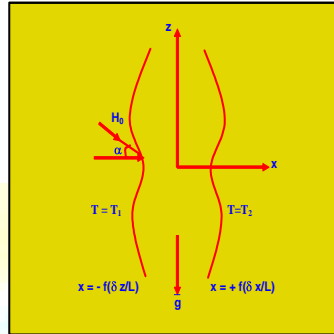
It has been established that channels with diverging – converging geometries augment the transportation of heat transfer and momentum. As the fluid flows through a tortuous path viz., the dilated – constricted geometry, there will be more intimate contact between them. The flow takes place both axially (primary) and transversely (secondary) with the secondary velocity being towards the axis in the fluid bulk rather than confining within a thin layer as in straight channels. Hence it is advantageous to go for converging-diverging geometries for improving the design of heat transfer equipment. This problem has been extended to the case of wavy walls Deshikachar et al [1]. Hyan Gook Won *et. al.*, [2] have analyzed that the flow and heat/mass transfer in a wavy duct with various corrugation angles in two dimensional flow regimes. Mahdy *et. al.*, [3] have studied the mixed convection heat and mass transfer on a vertical wavy plate embedded in a saturated porous media (PST/PSE) Comini *et. al.*, [4] have analyzed the convective heat and mass transfer in wavy finned-tube exchangers. Jer-Huan Jang *et. al.*, [5] have analyzed that the mixed convection heat and mass transfer along a vertical wavy surface.

Alam *et. al.*, [6] have studied unsteady free convective heat and mass transfer flow in a rotating system with Hall currents, viscous dissipation and Joule heating. Taking Hall effects in to account Krishan *et. al.*, [7] have investigated Hall effects on the unsteady hydromagnetic boundary layer flow. Siva Prasad *et. al.*, [8] have studied Hall effects on unsteady MHD free and forced convection flow in a porous rotating channel. The above work was done in effects in the unsteady cases has been studied in the recent times by a few authors [9-13].

FORMULATION OF THE PROBLEM

We consider the steady flow of an incompressible, viscous, electrically conducting fluid confined in a vertical channel bounded by two wavy walls under the influence of an inclined magnetic field of intensity H_0 lying in the plane (y-z). The magnetic field is inclined at an angle α to the axial direction k and hence its components are $(0, H_0 \sin(\alpha), H_0 \cos(\alpha))$. In view of the waviness of the wall the velocity field has components $(u, 0, w)$. The magnetic field in the presence of fluid

flow induces the current $(J_x, 0, J_z)$. We choose a rectangular cartesian co-ordinate system $O(x, y, z)$ with z-axis in the vertical direction and the walls at $x = \pm f(\frac{\delta z}{L})$.



Configuration of the Problem

When the strength of the magnetic field is very large we include the Hall current so that the generalized Ohm's law is modified to

$$\bar{J} + \omega_e \tau_e \bar{J} \times \bar{H} = \sigma (\bar{E} + \mu_e \bar{q} \times \bar{H}) \quad (1)$$

where \bar{q} is the velocity vector. \bar{H} is the magnetic field intensity vector \bar{E} is the electric field, \bar{J} is the current density vector, ω_e is the cyclotron frequency, τ_e is the electron collision time, σ is the fluid conductivity and μ_e is the magnetic permeability. Neglecting the electron pressure gradient-slip and thermo-electric effects and assuming the electric field $\bar{E}=0$,

$$j_x - m H_0 J_z \sin(\alpha) = -\sigma \mu_e H_0 w \sin(\alpha) \quad (2)$$

$$J_z + m H_0 J_x \sin(\alpha) = \sigma \mu_e H_0 u \sin(\alpha) \quad (3)$$

where $m = \omega_e \tau_e$ is the Hall parameter.

On solving equations (2)&(3) we obtain

$$j_x = \left(\frac{\sigma \mu_e H_0 \sin(\alpha)}{1 + m^2 H_0^2 \sin^2(\alpha)} \right) \left(m H_0 \sin(\alpha) - w \right) \quad (4)$$

$$j_z = \left(\frac{\sigma \mu_e H_0 \sin(\alpha)}{1 + m^2 H_0^2 \sin^2(\alpha)} \right) \left(+ m H_0 w \sin(\alpha) \right) \quad (5)$$

where u, w are the velocity components along x and z directions respectively,

The Momentum equations are

$$\left(u \frac{\partial u}{\partial x} + w \frac{\partial u}{\partial z} \right) = - \left(\frac{\partial p}{\partial x} \right) + \mu \left(\frac{\partial^2 u}{\partial x^2} + \frac{\partial^2 u}{\partial z^2} \right) + \mu_e \left(H_0 J_z \sin(\alpha) \right) - \rho \bar{g} \quad (6)$$

$$\left(u \frac{\partial W}{\partial x} + w \frac{\partial W}{\partial z}\right) = -\left(\frac{\partial p}{\partial z}\right) + \mu \left(\frac{\partial^2 W}{\partial x^2} + \frac{\partial^2 W}{\partial z^2}\right) + \mu_e \left(\frac{\partial J_x \sin(\alpha)}{\partial z}\right) \quad (7)$$

Substituting J_x and J_z from equations (4)&(5) in equations (6)&(7) we obtain

$$\left(u \frac{\partial u}{\partial x} + w \frac{\partial u}{\partial z}\right) = -\left(\frac{\partial p}{\partial x}\right) + \mu \left(\frac{\partial^2 u}{\partial x^2} + \frac{\partial^2 u}{\partial z^2}\right) - \left(\frac{\sigma \mu_e H_0^2 \sin^2(\alpha)}{1 + m^2 H_0^2 \sin^2(\alpha)}\right) \left(\frac{\partial w \sin(\alpha)}{\partial x}\right) \quad (8)$$

$$\left(u \frac{\partial W}{\partial x} + w \frac{\partial W}{\partial z}\right) = -\left(\frac{\partial p}{\partial z}\right) + \mu \left(\frac{\partial^2 W}{\partial x^2} + \frac{\partial^2 W}{\partial z^2}\right) - \left(\frac{\sigma \mu_e H_0^2 \sin^2(\alpha)}{1 + m^2 H_0^2 \sin^2(\alpha)}\right) \left(\frac{\partial w \sin(\alpha)}{\partial z} - \rho g\right) \quad (9)$$

The energy equation is

$$\rho C_p \left(u \frac{\partial T}{\partial x} + w \frac{\partial T}{\partial z}\right) = k_f \left(\frac{\partial^2 T}{\partial x^2} + \frac{\partial^2 T}{\partial z^2}\right) \quad (10)$$

The equation of state is

$$\rho - \rho_e = -\beta_0(T - T_e) - \beta_1(T - T_e)^2 \quad (11)$$

where T , is the temperature in the fluid. k_f is the thermal conductivity, C_p is the specific heat constant pressure, β is the coefficient of thermal expansion, Q is the strength of the heat source and q_r is the radiative heat flux.

The flow is maintained by a constant volume flux for which a characteristic velocity is defined as

$$q = \frac{1}{L} \int_{-L_f}^{L_f} w dx \quad (12)$$

The boundary conditions are

$$u=0, w=0, T=T_1, \text{ on } x = -f\left(\frac{\delta z}{L}\right) \quad (13)$$

$$w=0, u=0, T=T_2, \text{ on } x = f\left(\frac{\delta z}{L}\right) \quad (14)$$

Eliminating the pressure from equations(8)&(9) and introducing the Stokes Stream function ψ as

$$u = -\left(\frac{\partial \psi}{\partial z}\right), w = \left(\frac{\partial \psi}{\partial x}\right) \quad (15)$$

the equations (8)&(9), (15)&(11) in terms of ψ is

$$\left(\frac{\partial \psi}{\partial z} \frac{\partial (\nabla^2 \psi)}{\partial x} - \frac{\partial \psi}{\partial x} \frac{\partial (\nabla^2 \psi)}{\partial z}\right) = \mu \nabla^4 \psi + \beta_0 g \frac{\partial (T - T_e)}{\partial x} + 2\beta_1 g (T - T_e) \frac{\partial (T - T_e)}{\partial x} - \left(\frac{\sigma \mu_e^2 H_0^2 \sin^2(\alpha)}{1 + m^2 H_0^2 \sin^2(\alpha)}\right) \quad (16)$$

$$\rho C_p \left(\frac{\partial \psi}{\partial x} \frac{\partial T}{\partial z} - \frac{\partial \psi}{\partial z} \frac{\partial T}{\partial x}\right) = k_f \left(\frac{\partial^2 T}{\partial x^2} + \frac{\partial^2 T}{\partial z^2}\right) \quad (17)$$

On introducing the following non-dimensional variables

$$(x', z') = (x, z) / L, \quad \psi' = \frac{\psi}{qL}, \quad \theta = \frac{T - T_2}{T_1 - T_2}$$

the equation of momentum and energy in the non-dimensional form are

$$\nabla^4 \psi - M_1^2 \nabla^2 \psi + \frac{G}{R} \left(\frac{\partial \theta}{\partial x} + 2\gamma \theta \frac{\partial \theta}{\partial x} \right) = R \left(\frac{\partial \psi}{\partial z} \frac{\partial (\nabla^2 \psi)}{\partial x} - \frac{\partial \psi}{\partial x} \frac{\partial (\nabla^2 \psi)}{\partial z} \right) \quad (18)$$

$$PR \left(\frac{\partial \psi}{\partial x} \frac{\partial \theta}{\partial z} - \frac{\partial \psi}{\partial z} \frac{\partial \theta}{\partial x} \right) = \nabla^2 \theta - \alpha \quad (19)$$

where

$$G = \frac{\beta g \Delta T_e L^3}{\nu^2} \quad (\text{Grashof Number}) \quad M^2 = \frac{\sigma \mu_e^2 H_o^2 L^2}{\nu^2} \quad (\text{Hartman Number})$$

$$M_1^2 = \frac{M^2 \sin^2(\alpha)}{1+m^2} \quad R = \frac{qL}{\nu} \quad (\text{Reynolds Number})$$

$$P = \frac{\mu C_p}{K_f} \quad (\text{Prandtl Number}) \quad \gamma = \frac{\beta_1 (T_1 - T_2) L^3}{\beta_o} \quad (\text{Density ratio})$$

$$\alpha = \frac{QL^2}{\Delta TK_f} \quad (\text{Heat source parameter})$$

The corresponding boundary conditions are

$$\begin{aligned} \psi(f) - \psi(-f) &= 1 \\ \frac{\partial \psi}{\partial z} = 0, \frac{\partial \psi}{\partial x} = 0, \theta &= 1, \text{ at } x = -f(\delta z) \\ \frac{\partial \psi}{\partial z} = 0, \frac{\partial \psi}{\partial x} = 0, \theta &= 0 \text{ at } x = +f(\delta z) \end{aligned}$$

ANALYSIS OF THE FLOW

Introduce the transformation such that

$$\bar{x} = \delta x, \frac{\partial}{\partial x} = \delta \frac{\partial}{\partial \bar{x}} \quad (20)$$

$$\text{then } \frac{\partial}{\partial x} \approx O(\delta) \rightarrow \frac{\partial}{\partial \bar{x}} \approx O(1) \quad (21)$$

For small values of $\delta \ll 1$, the flow develops slowly with axial gradient of order δ and hence we

$$\text{take } \frac{\partial}{\partial \bar{x}} \approx O(1). \quad (22)$$

Using the above transformation the equations (20)-(22) reduce to

$$F^4 \psi - M_1^2 F^2 \psi + \frac{G}{R} \left(\frac{\partial \theta}{\partial x} + 2\gamma \theta \frac{\partial \theta}{\partial x} \right) = \delta R \left(\frac{\partial \psi}{\partial \bar{z}} \frac{\partial (F^2 \psi)}{\partial x} - \frac{\partial \psi}{\partial x} \frac{\partial (F^2 \psi)}{\partial \bar{z}} \right) \quad (23)$$

$$\delta PR \left(\frac{\partial \psi}{\partial x} \frac{\partial \theta}{\partial \bar{z}} - \frac{\partial \psi}{\partial \bar{z}} \frac{\partial \theta}{\partial x} \right) = F^2 \theta + \alpha \quad (24)$$

$$\text{where } F^2 = \frac{\partial}{\partial x^2} + \delta^2 \frac{\partial}{\partial \bar{z}^2} \quad (25)$$

Assuming the slope δ of the wavy boundary to be small we take

$$\begin{aligned} \psi(x, z) &= \psi_0(x, y) + \delta \psi_1(x, z) + \delta^2 \psi_2(x, z) + \dots \dots \dots \\ \theta(x, z) &= \theta_0(x, z) + \delta \theta_1(x, z) + \delta^2 \theta_2(x, z) + \dots \dots \dots \end{aligned} \quad (26)$$

Let $\eta = \frac{x}{f(\bar{z})}$ (27)

Substituting (25) in equations (23)&(24) and using (26) and equating the like powers of δ the equations and the respective boundary conditions to the zeroth order are

$$\frac{\partial^2 \theta_0}{\partial \eta^2} = (\alpha f^2) \tag{28}$$

$$\frac{\partial^4 \psi_0}{\partial \eta^4} - M_1^2 f^2 \frac{\partial^2 \psi_0}{\partial \eta^2} = -\frac{Gf^3}{R} \left(\frac{\partial \theta_0}{\partial \eta} + 2\gamma \theta_0 \frac{\partial \theta_0}{\partial \eta} \right) \tag{29}$$

with

$$\left. \begin{aligned} \psi_0(+1) - \psi_0(-1) &= 1 \\ \frac{\partial \psi_0}{\partial \eta} = 0, \frac{\partial \psi_0}{\partial \bar{z}} = 0, \theta_0 &= 1 \quad \text{at } \eta = -1 \\ \frac{\partial \psi_0}{\partial \eta} = 0, \frac{\partial \psi_0}{\partial \bar{z}} = 0, \theta_0 &= 0 \quad \text{at } \eta = +1 \end{aligned} \right\} \tag{30}$$

and to the first order are

$$\frac{\partial^2 \theta_1}{\partial \eta^2} = P Rf \left(\frac{\partial \psi_0}{\partial \eta} \frac{\partial \theta_0}{\partial \bar{z}} - \frac{\partial \psi_0}{\partial \bar{z}} \frac{\partial \theta_0}{\partial \eta} \right) \tag{31}$$

$$\frac{\partial^4 \psi_1}{\partial \eta^4} - M_1^2 f^2 \frac{\partial^2 \psi_1}{\partial \eta^2} = -\frac{Gf^3}{R} \left(\frac{\partial \theta_1}{\partial \eta} + 2\gamma (\theta_0 \frac{\partial \theta_1}{\partial \eta} + \theta_1 \frac{\partial \theta_0}{\partial \eta}) \right) + Rf \left(\frac{\partial \psi_0}{\partial \eta} \frac{\partial^3 \psi_0}{\partial \bar{z}^3} - \frac{\partial \psi_0}{\partial \bar{z}} \frac{\partial^3 \psi_0}{\partial x \partial \bar{z}^2} \right) \tag{32}$$

with

$$\left. \begin{aligned} \psi_1(+1) - \psi_1(-1) &= 0 \\ \frac{\partial \psi_1}{\partial \eta} = 0, \frac{\partial \psi_1}{\partial \bar{z}} = 0, \theta_1 &= 0, \quad \text{at } \eta = -1 \\ \frac{\partial \psi_1}{\partial \eta} = 0, \frac{\partial \psi_1}{\partial \bar{z}} = 0, \theta_1 &= 0 \quad \text{at } \eta = +1 \end{aligned} \right\} \tag{33}$$

NUSSELT NUMBER

The rate of heat transfer (Nusselt Number) on the walls has been calculated using the formula

$$Nu = \frac{1}{f(\theta_m - \theta_w)} \left(\frac{\partial \theta}{\partial \eta} \right)_{\eta=\pm 1} \quad \text{where } \theta_m = 0.5 \int_{-1}^1 \theta d\eta, \quad \theta_w = b_{57} + \delta b_{58}$$

$$(Nu)_{\eta=+1} = \frac{1}{f\theta_m} (a_{54} + \delta b_{56}), (Nu)_{\eta=-1} = \frac{1}{f(\theta_m - 1)} (b_{54} + \delta b_{55})$$

DISCUSSION OF THE NUMERICAL RESULTS

The actual axial flow is in vertically upwards direction and therefore $w > 0$ represents the actual flow. $w < 0$ represents a reversal flow in flow region. The variation of w with M shows that w exhibits a reversal flow in the entire region for $M \geq 4$ and the region of reversal flow enlarges with increasing M the magnitude of w reduces with $M \leq 4$ and enhances with $M \geq 10$ (fig.1). The variation of w with Hall parameter m shows that w enhances with m in entire flow region (fig.2). We notice the enhancement the axial velocity w with increase in heat source parameter α thus the presence of heat sources in the fluid region enhances w . The influence of the surface geometry on w is shown in fig.3. It is found that higher the constriction of the channel walls lesser w in the flow region (fig.4). The variation of w with density ratio γ is shown in fig.5. It is noticed that higher the density ratio γ larger w in flow region. An increase in inclination λ of the magnetic field reduces remarkable $|w|$ in the flow region (fig.6).

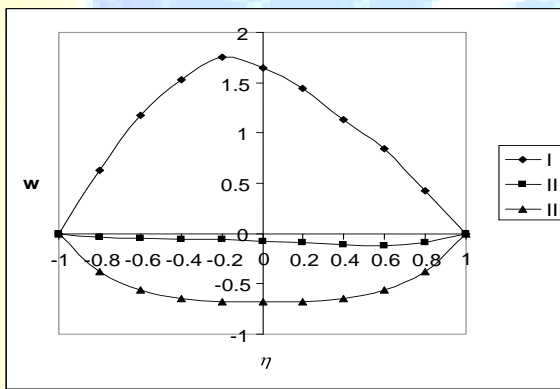


Fig. 1 : Variation of w with M
 $R=35, m=0.5, \alpha=2, \beta=-0.5, \gamma=0.5, \lambda=0.5$

M	I	II	III
	2	4	10

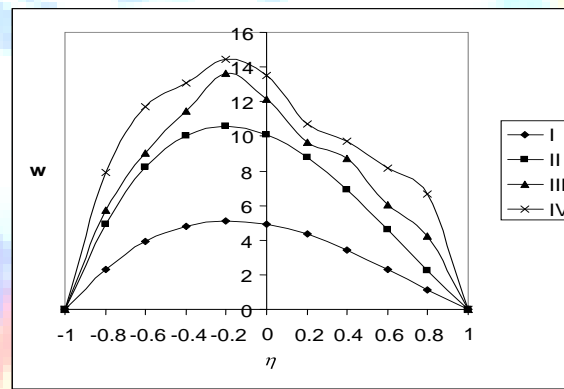


Fig. 2 : Variation of w with m
 $G=10^3, M=2, \alpha=2, \beta=-0.5, \gamma=0.5, \lambda=0.5$

m	I	II	III	IV
	0.5	1.5	2.5	3.5

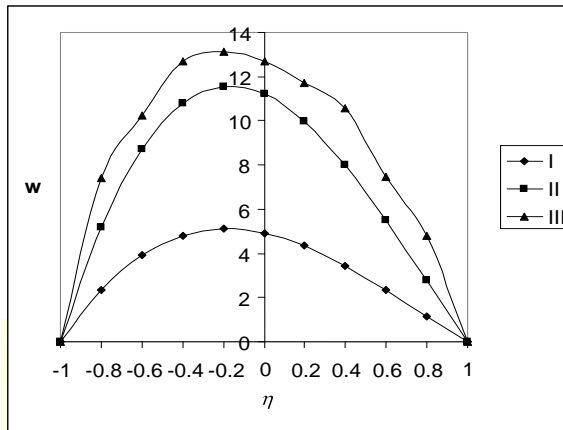


Fig. 3: Variation of w with α
 $R=35, M=2, m=0.5, \beta=-0.5, \gamma=0.5, \lambda=0.5$

	I	II	III
α	2	4	6

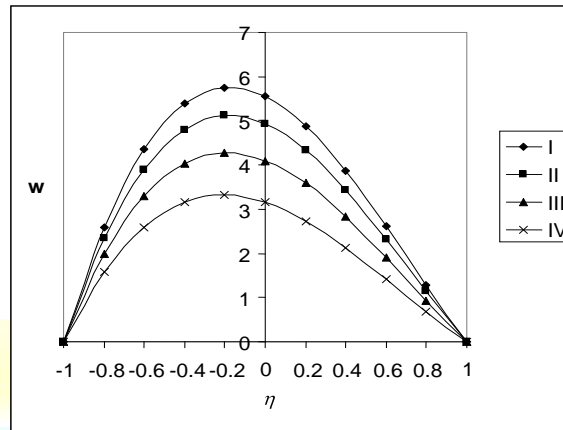


Fig. 4: Variation of w with β
 $G=10^3, M=2, m=0.5, \alpha=2, \gamma=0.5, \lambda=0.5$

	I	II	III	IV
β	-0.3	-0.5	-0.7	-0.9

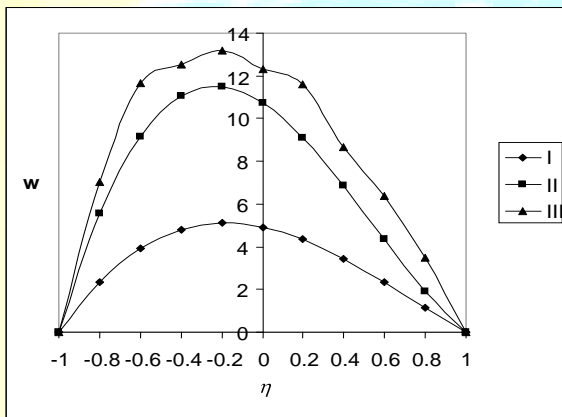


Fig. 5: Variation of w with γ
 $R=35, M=2, m=0.5, \alpha=2, \beta=-0.5, \lambda=0.5$

	I	II	III
γ	0.5	1.5	3.5

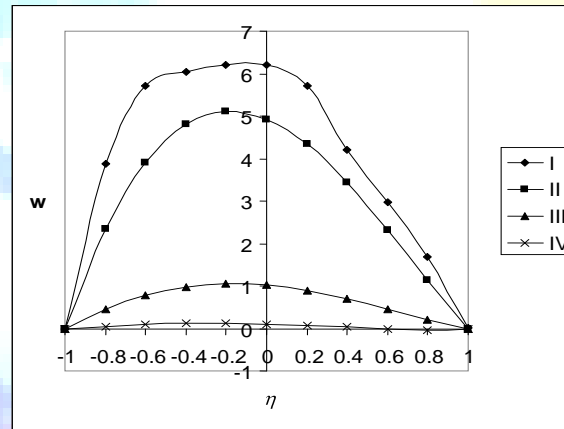


Fig. 6: Variation of w with λ
 $G=10^3, M=2, m=0.5, \alpha=2, \beta=-0.5, \gamma=0.5, x=\pi/4$

	I	II	III	IV
λ	0.25	0.5	0.75	1.0

The secondary velocity u which is due to the waviness of the boundary is shown in figs. 10 – 18 for different parametric values. The variation of u with M shows that $|u|$ reduces with $M \leq 4$ and enhance with $M \geq 6$ (fig. 7). Also $|u|$ experience an enhancement with increase in Hall parameter m and heat source parameter α (fig.8 & 9). The variation of u with β shows that higher the constriction of the channel walls larger $|u|$ in the flow region (fig.10). Fig.11 represents the variation of u with density ratio γ . Higher the density ratio γ larger $|u|$ everywhere in the region. An increase in inclination λ of the magnetic field lesser $|u|$ in entire flow region (fig.12).

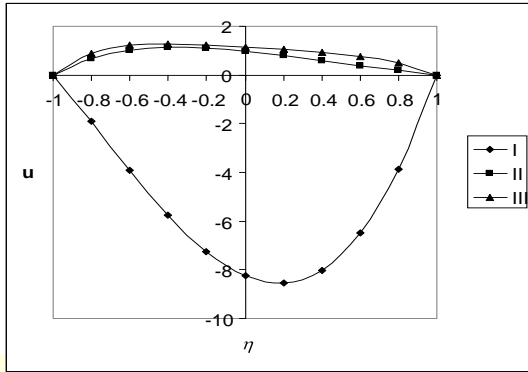


Fig. 7 : Variation of u with M
 $R=35, m=0.5, \alpha=2, \beta=-0.5, \gamma=0.5, \lambda=0.5$

	I	II	III
M	2	4	10

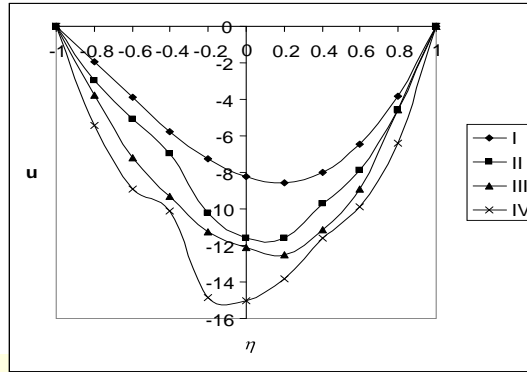


Fig. 8 : Variation of u with m
 $G=10^3, M=2, \alpha=2, \beta=-0.5, \gamma=0.5, \lambda=0.5$

	I	II	III	IV
m	0.5	1.5	2.5	3.5

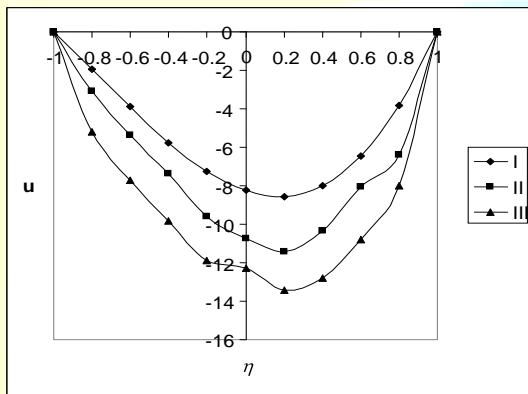


Fig. 9 : Variation of u with α
 $R=35, M=2, m=0.5, \beta=-0.5, \gamma=0.5, \lambda=0.5$

	I	II	III
α	2	4	6

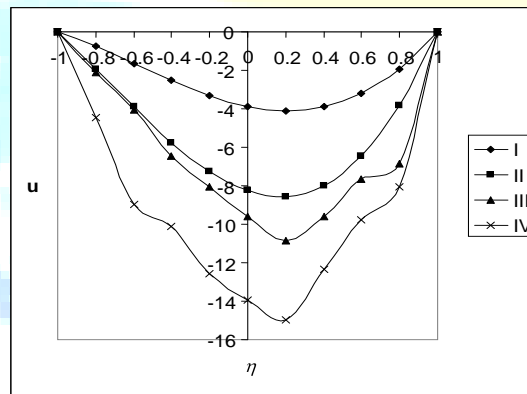


Fig. 10 : Variation of u with β
 $G=10^3, M=2, m=0.5, \alpha=2, \gamma=0.5, \lambda=0.5$

	I	II	III	IV
β	-0.3	-0.5	-0.7	-0.9

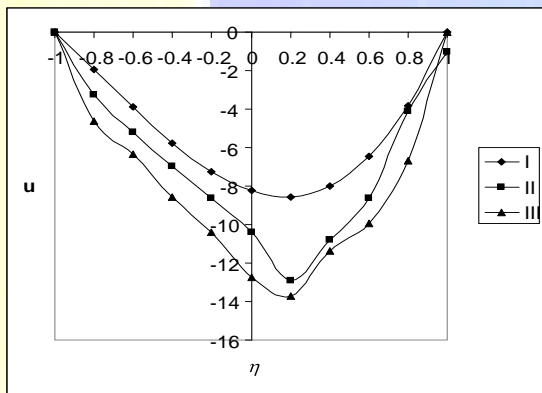


Fig. 11 : Variation of u with γ
 $R=35, M=2, N_1=0.5, \alpha=2, \beta=-0.5, \lambda=0.5$

	I	II	III
γ	0.5	1.5	3.5

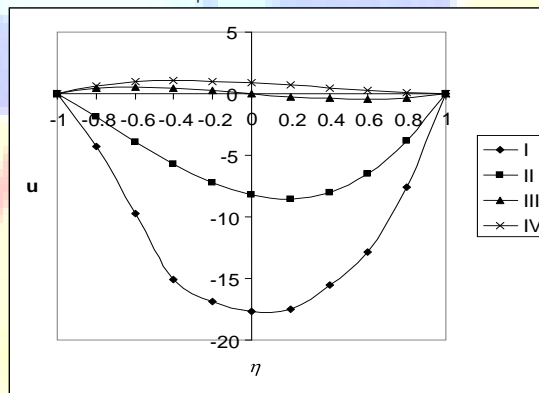


Fig. 12 : Variation of u with λ
 $G=10^3, M=2, m=0.5, \alpha=2, \beta=-0.5, \gamma=0.5, x=\pi/4$

	I	II	III	IV
λ	0.25	0.5	0.75	1.0

The non – dimensional temperature θ is shown in figures 13 – 18 for different parametric values . Higher the Lorentz force larger the actual temperature in flow region (fig.13). Fig. 14 represents the variation of θ with Hall parameter m . It shows that the actual temperature depreciation with increase in $m \leq 1.5$ and enhances with $m \geq 2.5$. Fig.15 represents the variation of θ with heat source parameter α we find that with the presence of

heat generating sources in the fluid region the actual temperature exhibits an increasing tendency with α . The variation of θ with β shows that higher the constriction of the channel walls lesser the actual temperature in the flow region (fig.16). Fig. 17 represents an increase in γ results in a depreciation in actual temperature. Fig.18 represents we find that an increase in the inclination λ of the inclined magnetic field reduces remarkable with $\lambda \leq 0.5$ and again enhances with $\lambda \geq 0.75$.

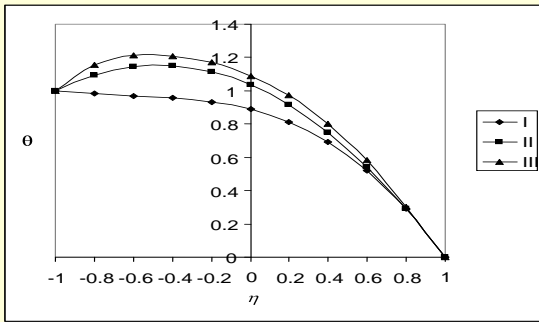


Fig. 13 : Variation of θ with M
 $R=35, m=0.5, \alpha=2, \beta=-0.5, \gamma=0.5, \lambda=0.5$

I	II	III	
M	2	4	10

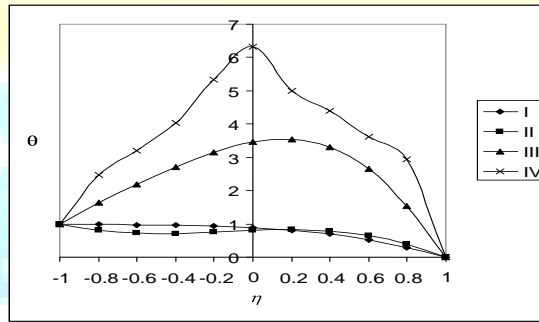


Fig. 14 : Variation of θ with m
 $G=10^3, M=2, \alpha=2, \beta=-0.5, \gamma=0.5, \lambda=0.5$

I	II	III	IV	
m	0.5	1.5	2.5	3.5

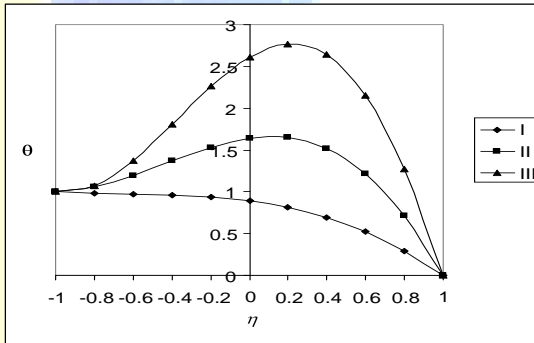


Fig. 15 : Variation of θ with α
 $R=35, M=2, m=0.5, \beta=-0.5, \gamma=0.5, \lambda=0.5$

I	II	III	
α	2	4	6

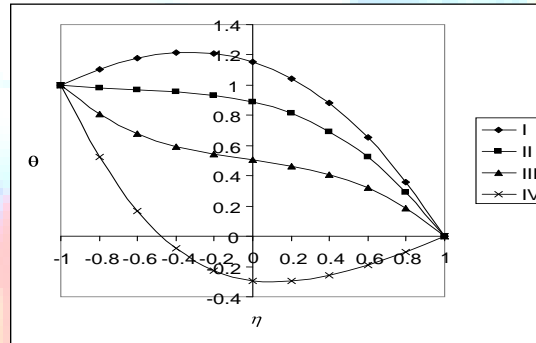


Fig. 16 : Variation of θ with β
 $G=10^3, M=2, m=0.5, \alpha=2, \gamma=0.5, \lambda=0.5$

I	II	III	IV	
β	-0.3	-0.5	-0.7	-0.9

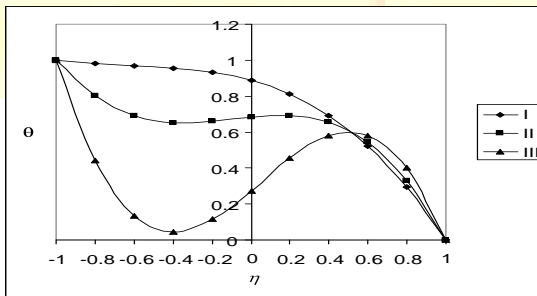


Fig. 17 : Variation of θ with γ
 $R=35, M=2, m=0.5, \alpha=2, \beta=-0.5, \lambda=0.5$

I	II	III	
γ	0.5	1.5	3.5

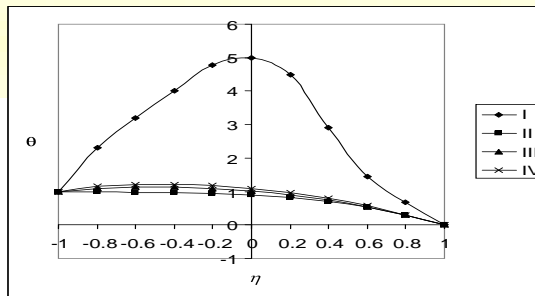


Fig. 18 : Variation of θ with λ
 $G=10^3, M=2, m=0.5, \alpha=2, \beta=-0.5, \gamma=0.5, x=\pi/4$

I	II	III	IV	
λ	0.25	0.5	0.75	1.0

The average Nusselt number (Nu) which measures the rate of heat transfer at $\eta = \pm 1$ is shown in tables. 1 – 6 for different parametric values. The variation of Nu with Hartmann number M shows that at $\eta = +1$ higher the Lorentz force lesser $|Nu|$ for all G, while $\eta = -1$, $|Nu|$ enhances with M in heating case and in cooling case it reduces with $M \leq 5$ and enhance with $M \geq 10$. The variation of Nu with Hall parameter ‘m’ reveals that at $\eta = +1$, $|Nu|$ enhances with $m \leq 2.5$ and reduces with $m \geq 3.5$. While $\eta = -1$ the rate of heat transfer enhance with lower and higher values of m and reduces with intermediate values of m for all G (tables.1&2). An increase in the strength of the heat source leads to an enhancement in the rate of heat transfer at $\eta = \pm 1$. The variation of Nu with wall waviness β shows that higher the constriction of the channel walls larger $|Nu|$ for $G > 0$ and for $G < 0$ lesser $|Nu|$ and further higher constriction larger $|Nu|$ for all G. The variation of Nu with γ shows that the rate of heat transfer enhances with increase in γ for $G > 0$ and reduces for $G < 0$. (tables. 3 & 4). An increase in the inclination of the magnetic field reduces $|Nu|$ in heating case and enhances in cooling case at $\eta = +1$ while at $\eta = -1$ it enhances with λ for all G (tables. 5&6).

TABLE .1 NUSSELT NUMBER (NU) AT $\eta = +1$

G	I	II	III	IV	V	VI
1×10^2	-1.07459	-0.91970	-0.94163	-1.70696	-1.73929	-0.56510
1×10^3	-1.56798	-0.91792	-0.94131	-4.63158	-1.96401	-0.56871
-1×10^2	-0.76445	-0.92148	-0.94194	-0.26715	-3.01496	-0.57614
-1×10^3	-0.55145	-0.92324	-0.94226	0.58967	-2.32738	-0.57239

TABLE .2 NUSSELT NUMBER (NU) AT $\eta = -1$

G	I	II	III	IV	V	VI
1×10^2	-0.23253	0.81946	0.87348	-3.08733	0.88180	2.46328
1×10^3	-8.26421	0.81513	0.87299	58.00443	0.93961	2.46905
-1×10^2	1.35056	0.82376	0.87397	2.37713	1.08655	2.48051
-1×10^3	2.02670	0.82804	0.87446	3.98767	1.00699	2.47480
M	2	5	10	2	2	2
m	0.5	0.5	0.5	1.5	2.5	3.5

TABLE . 3 NUSSELT NUMBER (NU) AT $\eta = +1$

G	I	II	III	IV	V	VI	VII
1×10^2	-1.63300	-1.96962	-1.05428	-1.06071	-8.89298	-0.99539	-0.92148
1×10^3	-2.57805	-2.83772	-1.22211	-10.47038	-1.26817	-1.22789	-0.96176
-1×10^2	-0.28873	1.54186	-0.90725	-0.68515	-0.90301	-0.82395	-0.88712
-1×10^3	1.77550	-15.41063	-0.77739	-0.55321	-0.99754	-0.69229	-0.85747

TABLE

.4

NUSSELT NUMBER (NU) AT $\eta = -1$

G	I	II	III	IV	V	VI	VII
1×10^2	0.04298	-0.16738	0.69333	-720.18830	2.52264	0.18363	0.52747

1×10^{-3}	-1.25265	-0.86127	0.04062	3.9626600	2.10035	-2.19472	-0.11316
-1×10^2	2.40451	7.10725	1.18345	1.577310	1.53583	1.16312	0.94864
-1×10^3	8.06646	-4.05555	1.56498	2.172180	1.78302	1.69743	1.24672
α	4	6	2	2	2	2	2
β	-0.5	-0.5	-0.3	-0.7	-0.9	-0.5	-0.5
γ	0.5	0.5	0.5	0.5	0.5	0.3	0.1

TABLE .5 NUSSELT NUMBER (NU) AT $\eta = +1$

G	I	II	III
1×10^2	-0.56510	-0.91648	-0.91607
1×10^3	-0.56871	-0.91870	-0.91214
-1×10^2	-0.57614	-0.91438	-0.91983
-1×10^3	-0.57239	-0.91239	-0.92360

TABLE .6 NUSSELT NUMBER (NU) AT $\eta = -1$

G	I	II	III
1×10^2	2.46328	0.74546	0.80252
1×10^3	2.46905	0.61331	0.77901
-1×10^2	2.48051	0.86106	0.82534
-1×10^3	2.47480	0.96289	0.84750
λ	0.25	0.75	1.0

CONCLUSIONS

The effect of radiation, dissipation and quadratic density temperature variation on convective heat transfer flow of a viscous, electrically conducting fluid in a vertical channel in the presence of heat sources. The important conclusions are following:

(1) The variation of w with M shows that w exhibits a reversal flow in the entire region for $M \geq 4$ and the region of reversal flow enlarges with increasing M the magnitude of w reduces with $M \leq 4$ and enhances with $M \geq 10$. The variation of w with Hall parameter m shows that w enhances with m in entire flow region. We notice the enhancement the axial velocity w with increase in heat source parameter α thus the presence of heat sources in the fluid region enhances w .

(2) The variation of u with M shows that $|u|$ reduces with $M \leq 4$ and enhance with $M \geq 6$. Also $|u|$ experience an enhancement with increase in Hall parameter m and heat source

parameter α . The variation of u with β shows that higher the constriction of the channel walls larger $|u|$ in the flow region. The variation of u with density ratio γ , higher the density ratio γ larger $|u|$ everywhere in the region. An increase in inclination λ of the magnetic field lesser $|u|$ in entire flow region.

(3) The variation of θ with Hall parameter m . It shows that the actual temperature depreciation with increase in $m \leq 1.5$ and enhances with $m \geq 2.5$. The variation of θ with heat source parameter α we find that with the presence of heat generating sources in the fluid region the actual temperature exhibits an increasing tendency with α . The variation of θ with β shows that higher the constriction of the channel walls lesser the actual temperature in the flow region.

(4) The variation of Nu with Hartmann number M shows that at $\eta = +1$ higher the Lorentz force lesser $|Nu|$ for all G , while $\eta = -1$, $|Nu|$ enhances with M in heating case and in cooling case it reduces with $M \leq 5$ and enhance with $M \geq 10$. The variation of Nu with Hall parameter 'm' reveals that at $\eta = +1$. $|Nu|$ enhances with $m \leq 2.5$ and reduces with $m \geq 3.5$. While $\eta = -1$ the rate of heat transfer enhance with lower and higher values of m and reduces with intermediate values of m for all G .

(5) The variation of Nu with wall waviness β shows that higher the constriction of the channel walls larger $|Nu|$ for $G > 0$ and for $G < 0$ lesser $|Nu|$ and further higher constriction larger $|Nu|$ for all G . The variation of Nu with γ shows that the rate of heat transfer enhances with increase in γ for $G > 0$ and reduces for $G < 0$. An increase in the inclination of the magnetic field reduces $|Nu|$ in heating case and enhances in cooling case at $\eta = +1$ while at $\eta = -1$ it enhances with λ for all G .

REFERENCES

- [1] Deshikachar,K.S and Ramachandra Rao,A: Int. J.Engg. Sci, 23(1985)1121.
- [2] Hyen Gook Wan,Sang Dong Hwang,Hyung He Cho:Heat and Mass transfer,45(2008) 157-165.
- [3] Mahdy,A: Int.J.Appl.Maths and Mech, 5(7)(2008)88-97.
- [4] Comini.G,Nomino.C and Savino.S : Int.J.Num.Methods for heat and fluid flow,12(6) (2002)735-755.
- [5] Jer-huan Jang and Wei-mon Yan: Int.J.heat and mass transfer ,47(2004)419-428.
- [6] Alam,M.M., and Sattar, M.A : J. of Energy heat and mass transfer, 22(2000) 31-39.
- [7] Krishna,D.V,Prasada rao,D.R.V,Ramachandra Murthy,A.S: J.Engg. Phy. and Thermo. Phy, 75(2)(2002)281-291.
- [8] Sivaprasad,R,Prasada Rao,D.R.V and Krishna,D.V: Ind.J. Pure and Appl. Maths, 19(2)(1988)688-696.
- [9] Krishna kumara, S.V.H.N, Ravi Kumar, Y.V.K and Ramana Murthy, M.V.: *Advances in Appl. Sci. Research*, 2(6)(2011) 439-453.
- [10] Raghunatha Rao T and Prasada Rao D R V, *Advances in Applied Science Research*, 3(4)(2012)2355-2368.
- [11] Rami Reddy, G and Venkata Ramana, S.: *Advances in Appl. Sci. Research*,2(5)(2011) 240-248.
- [12] Rathod, V.P. and Channakote, M.M.: R.: *Advances in Appl. Sci. Research*,2(3)(2011) 134-140.
- [13] Rathod, V.P. and Pallavi Kulkarni: *Advances in Appl. Sci. Research*, 2(3)(2011) 265-279.